



The Role of a Dopamine-Dependent Limbic–Motor Network in Sensory Motor Processing in Parkinson Disease

Leah G. Mann^{1,2} , Mathieu Servant³, Kaitlyn R. Hay², Alexander K. Song^{1,2}, Paula Trujillo², Bailu Yan², Hakmook Kang², David Zald⁴, Manus J. Donahue², Gordon D. Logan¹, and Daniel O. Claassen²

Abstract

■ Limbic and motor integration is enabled by a mesial temporal to motor cortex network. Parkinson disease (PD) is characterized by a loss of dorsal striatal dopamine but relative preservation of mesolimbic dopamine early in disease, along with changes to motor action control. Here, we studied 47 patients with PD using the Simon conflict task and [¹⁸F]fallypride PET imaging. Additionally, a cohort of 16 patients participated in a single-blinded dextroamphetamine (dAMPH) study. Task performance was evaluated using the diffusion model for conflict tasks, which allows for an assessment of interpretable action control processes. First, a voxel-wise examination disclosed a negative relationship, such

that longer non-decision time is associated with reduced D₂-like binding potential (BP_{ND}) in the bilateral putamen, left globus pallidus, and right insula. Second, an ROI analysis revealed a positive relationship, such that shorter non-decision time is associated with reduced D₂-like BP_{ND} in the amygdala and ventromedial OFC. The difference in non-decision time between off-dAMPH and on-dAMPH trials was positively associated with D₂-like BP_{ND} in the globus pallidus. These findings support the idea that dysfunction of the traditional striatal–motor loop underlies action control deficits but also suggest that a compensatory parallel limbic–motor loop regulates motor output. ■

INTRODUCTION

Proficient action control is necessary for adept cognitive and motor function, where behavioral disinhibition can manifest with impulsive behaviors and motor impulsivity can manifest with gait dysfunction (Ahlskog, 2011; Weintraub et al., 2010). Inhibitory function and impulsivity are often assessed using cognitive neuroscience tools that probe action control in the face of conflicting stimulus–action representations. Dopamine has long been recognized as an important modulator of inhibitory control (Mink, 1996). Studies in healthy populations and those that suffer from addiction, obesity, and neurodegenerative disorders such as Parkinson disease (PD) confirm the role of dopamine in action control proficiency (Ruitenberg, van Wouwe, Wylie, & Abrahamse, 2021; Albrecht, Kareken, Christian, Dzemidzic, & Yoder, 2014; Jentsch & Pennington, 2014; Ghahremani et al., 2012; Ersche et al., 2011; Volkow, Wang, & Baler, 2011; Volkow et al., 2008).

Recent studies provide tentative evidence for limbic regulation of motor control. A functional limbic–motor loop connects the mesial temporal structures, including the hippocampus and amygdala, to the motor cortex via

the ventral striatum, substantia nigra, pallidum, and motor thalamus (Aoki et al., 2019). Although clinical investigations into the relevance of this limbic–motor network have generally been sparse, emerging studies of psychiatric disorders that manifest with motor symptoms (e.g., psychogenic nonepileptic seizures) have established a significant link between these two distinct but related brain systems (Amiri et al., 2021; Aybek et al., 2015; van der Kruis et al., 2012). Additionally, an imaging study of response inhibition in patients with PD has revealed mesocorticolimbic regulation of action control, as greater D₂-like binding potential (BP_{ND}) in the amygdala and hippocampus is associated with better motor inhibitory control (Mann et al., 2021).

PD is a neurodegenerative disorder characterized by dopamine dysfunction, for which pharmacological restoration of dopamine tone can dramatically improve motor function. One commonly encountered nonmotor symptom of PD with dopaminergic medication is impulsive compulsive behaviors (ICBs), whereby patients develop overactive participation in rewarding activities associated with sex, eating, gambling, and shopping (Ahlskog, 2011; Voon et al., 2011). Investigations into ICBs have established important distinctions in mesocorticolimbic systems, with these patients showing evidence of differences in dopamine receptor expression in the ventral striatum;

¹Vanderbilt University, Nashville, TN, ²Vanderbilt University Medical Center, Nashville, TN, ³Université de Franche-Comté, Besançon, France, ⁴Rutgers University, Newark, NJ

enhanced dopamine release in this region; greater mesolimbic metabolism in response to dopamine therapies; and altered connectivity among the midbrain, amygdala, and ventral striatum (Petersen et al., 2018; Stark, Smith, Lin et al., 2018; Stark, Smith, Petersen et al., 2018; Claassen et al., 2017; Steeves et al., 2009). These findings point to an association between mesial temporal dopamine and impulsivity in PD. Together, they offer a unique opportunity to assess the limbic–motor network and the effect of dopamine on this system by applying methods that assess D₂-like receptor status, dopamine release, and action control proficiency.

Patients with PD often show poor action control, and typically, impulsivity is accompanied by impaired response inhibition (Ruitenberg et al., 2021; Moeller, Barratt, Dougherty, Schmitz, & Swann, 2001). Unexpectedly, despite an impulsive behavioral state, patients with ICBs maintain proficient action control, demonstrated by better stopping ability on the stop-signal task as compared to either healthy controls or patients with PD without ICBs and fewer impulsive errors on the Simon conflict task as compared with patients with PD without ICBs (Claassen et al., 2015; Wylie et al., 2012). The mechanisms contributing to intact action control in some patients with PD are not well understood. However, recent developments in the modeling of the Simon conflict test may aid the ability to understand these unique observations as well as the mechanisms underlying action control in PD at large. The task is a speeded choice RT paradigm that requires participants to make a left or right button press solely based on the color of the stimulus. By introducing a congruent or noncongruent location of the stimulus relative to the button press, the paradigm evaluates the impact of interference and conflict resolution in action control (Simon, 1969; Simon & Rudell, 1967). The task assesses RT, accuracy, and the Simon effect, or the extent to which responses are faster and more accurate when the stimulus and response are in the same location (left hand and left screen presentation) than when the stimulus and action are on opposite sides. Conventional outcome measures of performance have focused on accuracy at fast RTs using conditional accuracy functions, which show accuracy data as a function of RT quantiles (Ulrich, Schröter, Leuthold, & Birngruber, 2015; Heitz, 2014). Inhibition during longer RTs is assessed by determining delta functions, which reflect the difference in RT quantiles between congruent and incongruent trials versus the average of RT quantiles between congruent and incongruent trials (Ulrich et al., 2015; De Jong, Liang, & Lauber, 1994). An extension of the diffusion decision model has been developed to account for processing in this task (Ratcliff, Smith, Brown, & McKoon, 2016; Ulrich et al., 2015). The advantage of this diffusion model for conflict tasks (DMC) is that it decomposes behavioral data into psychologically interpretable action control processes, allowing for quantification of distinct goal-directed and non-goal-directed elements (Servant, van Wouwe, Wylie,

& Logan, 2018; Ratcliff et al., 2016; Ulrich et al., 2015; White, Ratcliff, Vasey, & McKoon, 2010; Ratcliff & McKoon, 2008). These two processes, namely, an automatic process related to the task-irrelevant location of the stimulus and a controlled process related to the task-relevant color of the stimulus, converge at the decision level and determine one's performance on the conflict task.

The DMC assumes that after stimulus presentation, noisy samples of evidence related to the color of the stimulus accumulate at rate v from a starting point z (fixed at zero) until a threshold $\pm a$. The upper threshold $+a$ corresponds to the correct response, and the lower threshold $-a$ corresponds to the incorrect response. The automatic process in correct congruent trials produces facilitation, and in incorrect incongruent trials, it produces interference. The resulting automatic activation is modeled by a rescaled gamma function with shape α (fixed at two), maximum amplitude $\pm\zeta$ (positive in congruent trials, negative in incongruent trials), and peak latency τ (Ulrich et al., 2015). In each trial, the predicted RT corresponds to (1) the decision time or the latency between accumulation onset and the first crossing of a threshold for a motor response plus (2) the residual latency with mean non-decision time (Ter), reflecting stimulus encoding and response output processes.

We hypothesized that given the proposed model of the limbic–motor network, mesocorticolimbic regions and their dopaminergic pathways would modify non-decision processes. To test this, we first examined the relationship between DMC parameters and D₂-like BP_{ND} as determined using the PET ligand [¹⁸F]fallypride, a high-affinity D_{2/3} receptor ligand. This imaging tool allows for the defining of striatal and extrastriatal D₂-like receptor status. We were therefore able to assess the relationship between dopamine and model-based components of action control, including non-decision time. Next, we assessed the relationship between dextroamphetamine (dAMPH) effects on DMC parameters and D₂-like BP_{ND} to localize where dAMPH exerts its effect. This was done in a 16-patient cohort who performed a single-blinded dAMPH administration protocol. dAMPH administration stimulates dopamine release, allowing for manipulation of dopamine quantities in vivo. At each visit (off-dAMPH or on-dAMPH), participants completed imaging with [¹⁸F]fallypride and the Simon conflict task. We related performance to dopamine release (dAMPH mediated changes to nondisplaceable BP_{ND}). We predicted that dopamine release (dAMPH condition) would speed RT by reducing non-decision time.

METHODS

Participants

Characteristic of PET studies is the limitation of sample size. In accordance with previous studies investigating [¹⁸F]fallypride PET BP_{ND} in relation to impulsivity and

related behavioral measures, we aimed for a sample size of $n = 18$ (Song et al., 2022; Mann et al., 2021; Stark, Smith, Lin et al., 2018). All patients with PD ($n = 47$, 16 women and 31 men) were recruited from the Movement Disorders Clinic at Vanderbilt University Medical Center. Patients met U.K. Brain Bank criteria for idiopathic PD (Hughes, Daniel, Kilford, & Lees, 1992) and had previously been diagnosed by a Movement Disorder Neurologist (D. C.). Prior to study commencement, all participants were screened to verify that they met inclusion and exclusion criteria. Patients were excluded from the study if they had an implanted deep brain stimulator, an unstable medical condition, a comorbid neurological disorder, dementia, a history of major psychiatric illness, or a history of substance abuse. Additionally, no patients had taken psychostimulants over the previous year, and none were currently using cocaine, nicotine, or excessive alcohol.

A physical exam, neurological exam, electrocardiogram, urinalysis, and metabolic panel were performed for all patients. Additionally, patients completed Part II of the Movement Disorders Society–United Parkinson’s Disease Rating Scale (MDS-UPDRS), which serves as a self-evaluation of motor activities of daily living, and Part III (in the off-medication condition), which serves as a clinician-scored motor examination (Weintraub et al., 2012; Goetz et al., 2008). Cognition was assessed with the Montreal Cognitive Assessment, and symptoms of depression were evaluated with the Center for Epidemiologic Studies Depression Scale–Revised. Lastly, the Questionnaire for Impulsive-Compulsive Disorders in Parkinson’s Disease–Rating Scale was administered to screen for ICBs. To confirm and further define the clinical presence of ICBs, semistructured interviews with patients and caregivers were performed, with an ICB designation based on previously described *DSM-5 (Diagnostic and Statistical Manual of Mental Disorders, Fifth Edition)* criteria (Voon et al., 2006).

Dopamine medications were converted to levodopa equivalent daily dose (Tomlinson et al., 2010). Following a 36-hr withdrawal from dopamine agonist therapy and a 16-hr withdrawal from levodopa therapy, participants ($n = 47$) attended a first testing visit in the off-medication state. This period was considered sufficient to eliminate effects from dopaminergic therapies while minimizing potential patient discomfort as the half-lives of levodopa and immediate-release dopamine agonists are ~ 1.5 and 6 hr, respectively (Tompson & Oliver-Willwong, 2009; Fabbrini, Juncos, Mouradian, Serrati, & Chase, 1987). In the cohort that completed the dAMPH challenge, they attended a second session during which they were administered a 0.43-mg/kg oral dose of dAMPH. The order of these visits was blinded to the participant only (i.e., single blind). The study was designed in this manner to prevent the influence of dAMPH on D_2 -like receptor BP_{ND} in the off-dAMPH state. Because the administration of amphetamine is understood to induce receptor internalization after treatment, it is imperative to begin with the off-dAMPH session to avoid any lingering effects of dAMPH (Buckholtz et al., 2010; Skinbjerg et al., 2010).

Table 1 presents demographic and clinical information. The study was carried out in accordance with the Declaration of Helsinki, and all participants provided written, informed consent before participating in the study in compliance with the standards of ethical conduct in human investigation regulated by the local institutional review board.

Simon Task

Participants performed a manual version of the Simon conflict task (Simon & Rudell, 1967). They wore corrective lenses if prescribed and were seated at a comfortable distance from a laptop screen and provided with directions before proceeding. They were instructed to make a left-hand button press to a green circle and a right-hand button

Table 1. Demographic and Clinical Evaluation of the Participants with PD

Variables	All Patients with PD	Patients with PD On-dAMPH (0.43 mg/kg Oral Dose)
<i>n</i>	47	16
Sex (male/female)	31/16	10/6
Age (years)	62.7 \pm 7.9	64.1 \pm 5.5
ICB (+/–)	24/23	9/7
Disease duration (years)	5.8 \pm 3.8	6 \pm 3.7
CES-D	15.7 \pm 9.1	16.3 \pm 10.6
MDS-UPDRS-II	19 \pm 9.1	13 \pm 8.7
MDS-UPDRS-III (Off)	29.3 \pm 11.7	30.2 \pm 12.6
Total LEDD (mg/day)	639.6 \pm 375.1	695.6 \pm 307.2
Agonist single dose equivalent (mg/day)	142.5 \pm 102.1	75.3 \pm 34.4

Data are shown as mean \pm standard deviation. CES-D = Center for Epidemiologic Studies Depression Scale; MDS-UPDRS = Movement Disorders Society–United Parkinson’s Disease Rating Scale; LEDD = Levodopa Equivalent Daily Dose.

press to a blue circle. Each trial consisted of a fixation point followed by a blue or green circle on either side of the screen. On corresponding trials, the circle was presented on the side of the screen that matched the correct response for its color. Accordingly, corresponding trials involved a green circle on the left side of the screen or a blue circle on the right side of the screen. On noncorresponding trials, the circle was presented on the side of the screen that did not match the correct response for its color. Accordingly, noncorresponding trials involved a green circle on the right side of the screen or a blue circle on the left side of the screen. Participants were asked to make their responses as quickly and accurately as possible. Once a choice had been executed or 1500 msec had elapsed, the trial ended. Each administration of the Simon conflict task involved 80 practice trials, followed by four blocks of 80 trials.

DMC Fitting Procedure

The DMC was coded in C and was simulated using a Euler-Maruyama approximation. The time step dt was fixed at 0.001 sec, and the diffusion was fixed at 0.1 to avoid complications arising from a scaling property of the model. The model was fit to each individual data set by minimizing the following likelihood ratio chi-square statistic G^2 :

$$G^2 = 2 \left(\sum_{i=1}^2 n_i \sum_{j=1}^{12} p_{ij} \log \frac{p_{ij}}{\pi_{ij}} \right)$$

The outer summation i extends over the two congruency conditions, and n_i represents the number of valid trials per condition. The inner summation j extends over the 12 bins bounded by 0.1, 0.3, 0.5, 0.7, and 0.9 RT quantiles for each pair of joint distributions of correct and error responses. When the number of errors Ne was low, we considered three RT quantiles (0.3, 0.5, 0.7) if $5 < Ne \leq 10$, and the median RT if $0 < Ne \leq 5$. Variables p_{ij} and π_{ij} represent the observed and predicted proportions of trials in RT bin j of congruency condition i . The G^2 statistic thus characterizes the goodness-of-fit of the model to the correct and error RT distributions and the correct and error choice probabilities simultaneously. The lower the G^2 , the higher the fit quality. It was minimized using a differential evolution optimizer and 30,000 simulated trials per congruency condition.

Although the DMC specifies the time course of the automatic activation, it is agnostic with respect to the mechanisms underlying both automaticity, which could include attentional selectivity or retrieval of instances in long-term memory, and its short-lived nature, which could include inhibition and passive decay (Ridderinkhof, 2002; Hommel, 1994; Logan, 1988). Following Ulrich et al., we further incorporated between-trial variability in the starting point of the evidence accumulation and residual latencies (Ulrich et al., 2015). We did not analyze between-trial variability parameters, however, as there is little theoretical justification for

them beyond improving the fit quality of the model, and their identifiability has not been assessed by parameter recovery studies (Minassian et al., 2016; Greenwald, Schuster, Johanson, & Jewell, 1998).

PET Imaging Protocol

[¹⁸F]fallypride was synthesized as outlined in a previously described method (Stark, Smith, Petersen et al., 2018). Data were collected on a Philips Vereos PET/CT scanner or a GE scanner with a three-dimensional acquisition and transmission attenuation correction. Approximately 2 hr after medication (placebo or dAMPH) administration, serial PET scans were acquired simultaneously with a 5.0-mCi bolus injection of [¹⁸F]fallypride over a 30-sec period. Scan time ran to approximately 3.5 hr postinjection with two breaks of 15 min between emission scans (Stark, Smith, Petersen, et al., 2018).

MRI Protocol

Anatomical T1-weighted MR images were acquired to allow region definition for ROI analyses and spatial normalization for voxel-wise analyses. All MRI scans were completed with a 3.0-T Philips MRI scanner with a body coil transmission and 32-channel SENSE array reception. Structural images were acquired using a T1-weighted high-resolution anatomical scan (MPRAGE; spatial resolution $1 \times 1 \times 1 \text{ mm}^3$; repetition time/echo time = 8.9/4.6 msec).

PET Image Processing

[¹⁸F]fallypride nondisplaceable binding potential (BP_{ND}) was quantified following motion correction with Statistical Parametric Mapping software (SPM12, Wellcome Trust Centre for Neuroimaging, <https://www.fil.ion.ucl.ac.uk/spm/software/>). Parametric BP_{ND} images were estimated using the simplified reference tissue model in PMOD software (PMOD Technologies; Stark, Smith, Petersen et al., 2018). The cerebellum was used as a reference region because of its limited D_{2/3} receptor expression (Camps, Cortés, Gueye, Probst, & Palacios, 1989). Parametric BP_{ND} images were co-registered to the participant's T1-weighted MR image using FSL's FLIRT with 6 degrees of freedom and a mutual information cost function (FSL v6.0, FMRIB). For voxel-level analyses, parametric BP_{ND} images were nonlinearly registered to standard Montreal Neurological Institute (MNI152) space using FSL's FNIRT.

ROI Analyses

A priori bilateral subcortical ROIs were manually defined on each participant's T1 MRI image according to established anatomical definitions (Stark, Smith, Petersen et al., 2018). These ROIs included the caudate (head), putamen, globus pallidus, ventral striatum, substantia

nigra, amygdala, and cerebellum. Additionally, the ventromedial OFC was manually defined according to proposed anatomical landmarks (Mackey & Petrides, 2009). The hippocampus and thalamus were segmented with FSL FIRST.

Analysis of Simon Task and D₂ BP_{ND} Data

All RT values fell below 1500 msec as a time limit had already been incorporated into the experiment. Thus, the only data trimming that was completed during preprocessing involved removing RTs that were less than 150 msec. First, a behavioral assessment of the Simon task data was performed to compute any differences in performance because of treatment or congruency conditions. A two-way repeated-measures ANOVA was applied to determine the possible effect of congruency and treatment on mean RT. Similarly, a two-way repeated-measures ANOVA was used to analyze the potential effect of congruency and treatment on mean accuracy.

To investigate the relationship between [¹⁸F]fallypride BP_{ND} and Simon task performance, a voxel-wise analysis was completed using SPM12. The regression of D₂ BP_{ND} on DMC parameters across cortical and subcortical areas included age, sex, and MDS-UPDRS-III (off) scores as covariates (Mukherjee et al., 2002; Pohjalainen, Rinne, Någren, Syvälahti, & Hietala, 1998). Significance criteria consisted of an uncorrected $p < .005$ and cluster-level false discovery rate (FDR) controlled at 0.05 to correct for multiple comparisons. Furthermore, a general linear model

(GLM) was applied to identify any additional correlations between [¹⁸F]fallypride BP_{ND} and DMC parameters. For this model, DMC parameters served as the dependent variable; mean ROI BP_{ND} as the independent variable; and age, sex, and MDS-UPDRS-III (off) scores as covariates. An FDR of 0.05 was used to correct for multiple comparisons (Benjamini & Hochberg, 1995). A robust linear model was also implemented to confirm significance.

Next, we sought to further characterize the interpretation of the ANOVA results, namely, that dAMPH regulates RT through its effect on non-decision time. To accomplish this, a GLM was used to define which, if any, of the DMC parameters was a predictor of change in mean RT. For this analysis, change in mean RT between off-dAMPH and on-dAMPH sessions served as the dependent variable; change in DMC parameters as the independent variable; and age, sex, and MDS-UPDRS-III (off) scores as covariates.

Finally, a GLM was used to test the hypothesis that D₂ receptor expression in striatal or extrastriatal regions may also contribute to distinct effects of dAMPH on Simon task performance. For this analysis, change in DMC parameters between off-dAMPH and on-dAMPH sessions served as the dependent variable; mean ROI BP_{ND} as the independent variable; and age, sex, and MDS-UPDRS-III (off) scores as covariates. Again, an FDR of 0.05 was used to correct for multiple comparisons. All statistical analyses were performed using R (R Foundation for Statistical Computing, 2016).

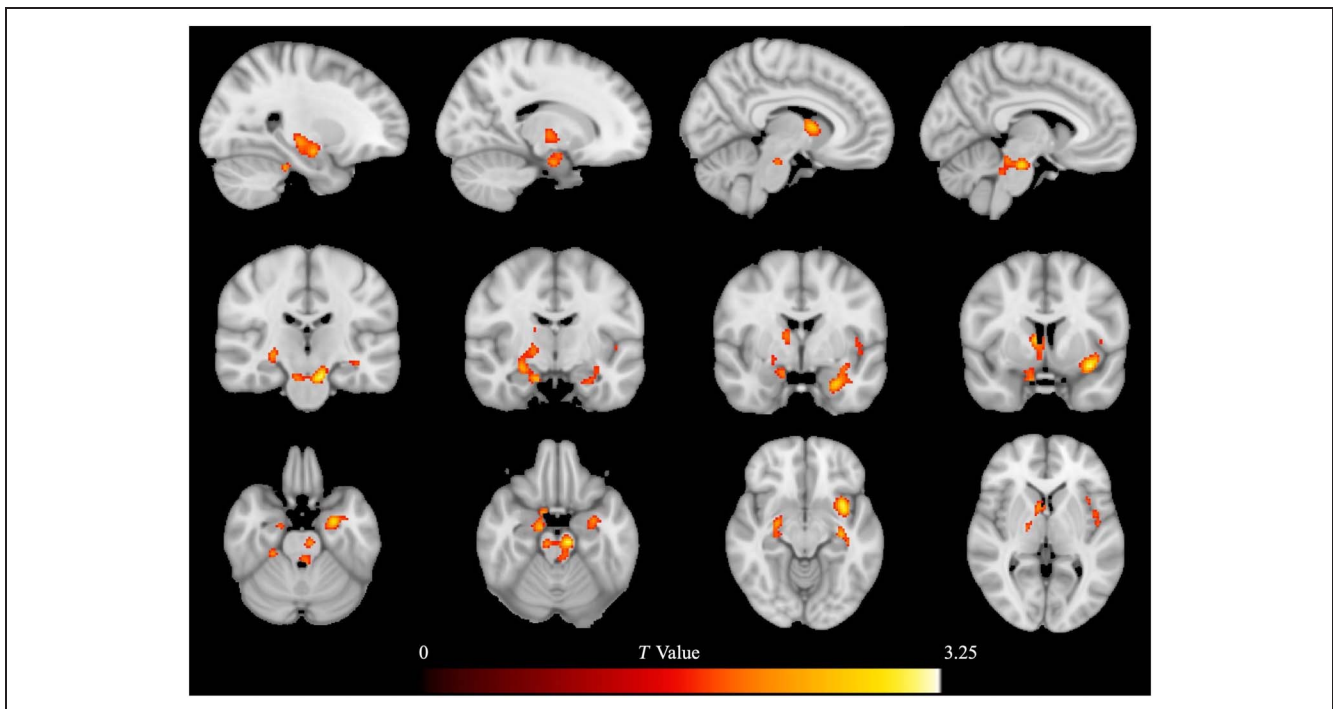


Figure 1. Voxel-wise regression of off-dAMPH [¹⁸F]fallypride BP_{ND} on off-dAMPH *Ter*. Map of clusters where *Ter* was positively correlated with [¹⁸F]fallypride BP_{ND} in patients with PD, overlaid on sagittal (top row), coronal (center row), and axial slices (bottom row) of a T1-weighted MNI brain template. Peaks for all clusters were significant at an uncorrected $p < .05$ but did not survive cluster-level FDR correction at $p < .05$. The clusters were localized to areas including the bilateral amygdala and hippocampus, right caudate, insular cortex, substantia nigra, and locus coeruleus.

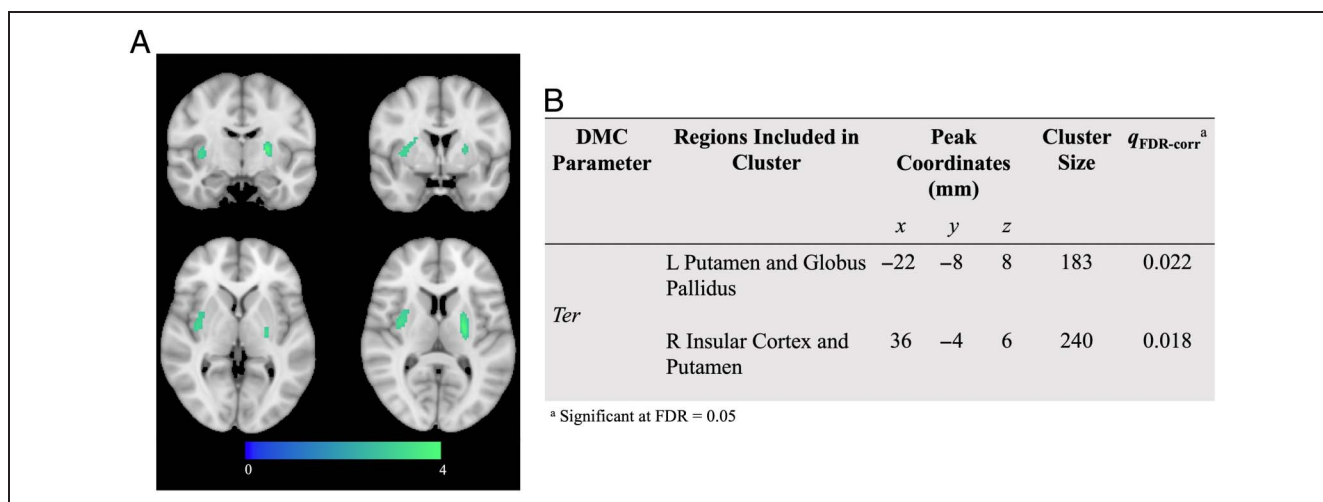


Figure 2. Voxel-wise regression of off-dAMPH [¹⁸F]fallypride BP_{ND} on off-dAMPH *Ter*. (A) Map of significant clusters where *Ter* was negatively correlated with [¹⁸F]fallypride BP_{ND} in patients with PD, overlaid on coronal and axial slices of an MNI template brain. All survived cluster-level FDR correction at $p < .05$. (B) Areas with a negative relationship with *Ter* include the bilateral putamen, left globus pallidus, and right insula.

RESULTS

Two Dissociable Relationships Between Off-dAMPH Mean Non-Decision Time and Off-dAMPH [¹⁸F]fallypride BP_{ND} in Basal Ganglia Regions and Mesial Temporal Areas

Employing a voxel-wise analysis on off-dAMPH data from all participants, we noted positive correlations between off-dAMPH [¹⁸F]fallypride BP_{ND} and *Ter*, or mean non-decision time, in several mesocortical regions. Clusters localized to the amygdala, hippocampus, insular cortex, right caudate, locus coeruleus, and substantia nigra, but these were not significant at an uncorrected height threshold of $p < .005$ and cluster-level FDR controlled at

0.05. Figure 1 shows these biologically relevant correlations.

The voxel-wise analysis also revealed a negative relationship, such that shorter non-decision time is associated with greater BP_{ND} in the bilateral putamen, left globus pallidus, and right insula. These two clusters remained significant following cluster-level FDR correction at 0.05 (left cluster $q_{FDR-corr} = 0.022$, right cluster $q_{FDR-corr} = 0.018$). Figure 2 displays the significant relationships between [¹⁸F]fallypride BP_{ND} and *Ter*. No significant clusters emerged for a relationship between off-dAMPH [¹⁸F]fallypride BP_{ND} and the remaining DMC parameters.

With an ROI-based approach, positive correlations between off-dAMPH [¹⁸F]fallypride BP_{ND} and off-dAMPH

Table 2. [¹⁸F]fallypride BP_{ND} (Off-dAMPH) Effects on DMC Parameter *Ter*

ROI	^[18F] fallypride BP _{ND} Mean ± SD	<i>Ter</i> ~ BP _{ND} + Age + Sex + UPDRS		
		95% CI	Coefficient	p^a (Adjusted p^b)
Ventral striatum	12.85 ± 2.89	[0.382, 10.361]	5.371	.036 (.080)
Caudate	15.63 ± 2.91	[-4.825, 6.863]	1.019	.727 (.727)
Putamen	20.69 ± 3.84	[-5.804, 2.679]	-1.563	.461 (.519)
Substantia nigra	1.12 ± 0.28	[8.721, 108.551]	58.636	.022 (.067)
Globus pallidus	11.23 ± 2.32	[-12.622, 0.483]	-6.070	.069 (.103)
Amygdala	1.67 ± 0.52	[15.882, 66.051]	40.966	.002 (.017 ^c)
Thalamus	1.74 ± 0.40	[-58.037, 20.063]	-18.987	.332 (.427)
Hippocampus	0.91 ± 0.23	[-3.605, 126.303]	61.349	.064 (.103)
Ventromedial OFC	2.97 ± 1.33	[5.180, 25.082]	15.131	.004 (.017 ^c)

GLM with FDR controlled at 0.05 to correct for multiple comparisons.

^a Uncorrected p value

^b FDR-corrected p value.

^c Significant FDR-corrected p value at .05.

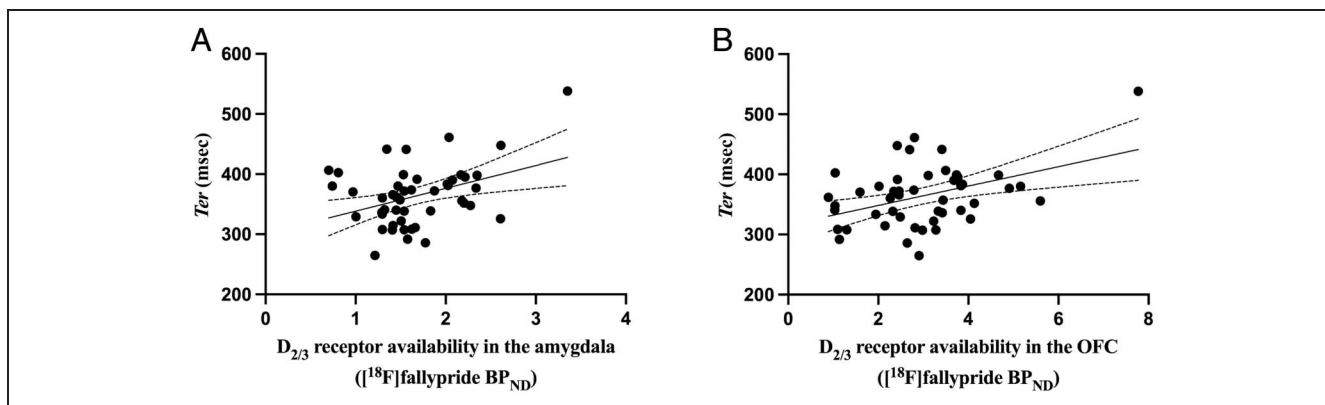


Figure 3. Scatterplots with lines of best fit displaying the relationship between off-dAMPH T_{er} and off-dAMPH $[^{18}\text{F}]\text{fallypride BP}_{\text{ND}}$. A GLM was applied with DMC parameters as the dependent variable and mean ROI BP_{ND} as the independent variable. Age, sex, and MDS-UPDRS-III (off) score served as covariates. A significant positive correlation between BP_{ND} and T_{er} (non-decision time) was observed for the (A) amygdala ($p = .017$) and the (B) OFC ($p = .017$), indicating a positive relationship between $D_{2/3}$ availability and mean non-decision time in these limbic areas. Additionally, a robust linear model confirmed significance for the amygdala and ventromedial OFC prior to FDR correction ($p_{\text{uncorrected}} = .035$, $p_{\text{uncorrected}} = .034$).

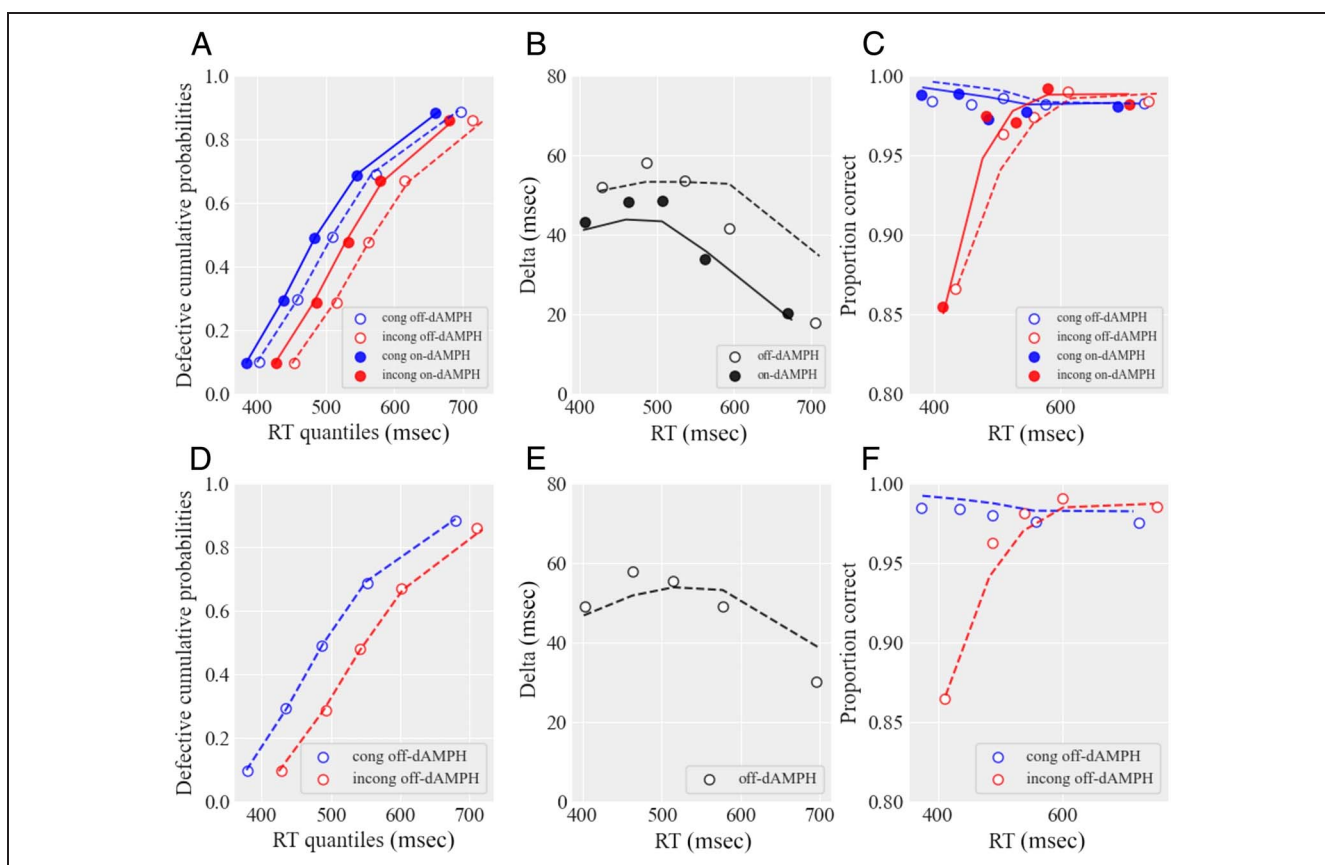


Figure 4. Observed data and DMC predictions averaged across participants. The data are shown as dots, and model predictions are shown as lines. For each participant and condition, model predictions were computed by simulating 100,000 trials. A–C depict data and model predictions for the 16 participants who completed both off-dAMPH and on-dAMPH conditions. D–F depict data and model predictions for all 47 participants who completed the off-dAMPH condition. (A, D) Observed versus predicted RT quantiles (0.1, 0.3, 0.5, 0.7, 0.9) of correct responses, weighted by the corresponding response proportion (defective cumulative RT distributions). (B, E) Observed versus predicted delta functions, constructed by plotting the difference (y axis) against the average (x axis) of equivalent RT quantiles of correct trials between incongruent and congruent conditions. (C, F) Observed versus predicted conditional accuracy functions, constructed by plotting the proportion of correct responses (y axis) against mean RT (x axis) in five RT bins of equal size. Note that conditional accuracy functions were not directly factored out in parameter estimation and can be considered as out-of-sample data. The good correspondence between data and model predictions strengthens the validity of model inferences.

DMC parameter, Ter , were found in extrastriatal ROIs, specifically in mesocorticolimbic regions. There were significant correlations between Ter and [^{18}F]fallypride BP_{ND} in the amygdala (coefficient = 40.966) and the ventromedial OFC (coefficient = 15.131). Both the amygdala and the ventromedial OFC remained significant following FDR correction for multiple comparisons at 0.05 ($p = .017$, $p = .017$). Moreover, the correlations between Ter and BP_{ND} in the substantia nigra and ventral striatum (coefficient = 58.636, coefficient = 5.371), showed a similar positive correlation but failed to reach FDR levels of significance ($p = .067$, $p = .080$). Table 2 presents mean regional [^{18}F]fallypride BP_{ND} values for all ROIs, along with 95% confidence intervals, coefficients, and p values from the GLM analysis between [^{18}F]fallypride BP_{ND} and Ter . Figure 3 displays the significant positive relationships between [^{18}F]fallypride BP_{ND} and Ter . No significant correlations between [^{18}F]fallypride BP_{ND} and the other DMC parameters emerged with the ROI analysis.

dAMPH Accelerates Simon Task Mean RT

The dAMPH challenge cohort consisted of 16 participants who completed both the off-medication off-dAMPH session and the off-medication on-dAMPH session. A repeated-measures ANOVA of Simon task performance in both off-dAMPH and on-dAMPH states revealed the classic effect of congruency on both mean RT ($p < .001$) and accuracy ($p = .009$). Consistent with previous findings of stimulant effects, dAMPH reduced mean RT ($p = .020$, effect size = 0.651) but did not affect accuracy ($p = .849$; Koelega, 1993; Mayfield, Randall, Spirduso, & Wilcox, 1993). Figure 4A shows that dAMPH produces a leftward shift of cumulative RT distributions compared to the off-dAMPH condition, suggesting that chronometric performance between the two states essentially differs by a constant. Interactions between congruency and treatment did not reach statistical significance (mean RT: $p = .615$; accuracy: $p = .885$).

Panels B and C of Figure 4 show delta and conditional accuracy functions for the 16 participants who completed

both off-dAMPH and on-dAMPH sessions, whereas panels E and F of Figure 4 show delta and conditional accuracy functions for all 47 participants. Delta functions decrease as RT increases, and conditional accuracy functions exhibit a dip in accuracy for fast RTs in incongruent trials. These trends, typically observed in the Simon task, do not appear to vary as a function of treatment (Ulrich et al., 2015; Ridderinkhof, 2002).

Effect of dAMPH on Mean RT Is Mediated by Non-Decision Time

Because the DMC parameters are implicated in the results, it is imperative to confirm that the model fits the data. Figure 4 shows a good correspondence between data and model predictions, suggesting that the DMC architecture is a plausible processing account of the data. Table 3 summarizes the best-fitting DMC parameters for the data averaged across participants. In the subset of participants ($n = 16$) completing both on-dAMPH and off-dAMPH conditions, dAMPH significantly lowered the non-decision time parameter ($p = .044$, effect size = 0.573), and showed a nonsignificant trend in lowering the amplitude of the automatic activation caused by the task-irrelevant location ($p = .070$, effect size = 0.381).

The GLM analysis of the relationship between change in mean RT and change in DMC parameters revealed significance for the mean non-decision time parameter, Ter (coefficient = 0.604). This relationship remained significant following FDR correction for multiple comparisons at 0.05 ($p = .021$). This positive correlation between the change in Ter and the change in mean RT indicates that as mean non-decision time decreases with dAMPH, so too does mean RT. Figure 5 displays the significant relationship between Ter change and mean RT change. Change in the other four DMC parameters in response to dAMPH did not show significant relationships with change in mean RT in response to dAMPH (v : coefficient = 76.972, $p = .451$; a : coefficient = 141.787, $p = .677$; ζ : coefficient = -224.531 , $p = .918$; τ : coefficient = 0.0673, $p = .483$).

Table 3. DMC Parameters Averaged across All Participants

DMC Parameters	Patients with PD Off-dAMPH ($n = 47$)	Patients with PD Off-dAMPH (Patients Who Performed dAMPH Challenge; $n = 16$)	Patients with PD On-dAMPH ($n = 16$)	p
v	0.393 \pm 0.11	0.402 \pm 0.14	0.452 \pm 0.17	.179
a	0.066 \pm 0.02	0.061 \pm 0.008	0.074 \pm 0.04	.438
Ter (msec)	364 \pm 50.6	397 \pm 50	362 \pm 65.8	.044 ^a
τ (msec)	142 \pm 182	118 \pm 174	96.9 \pm 121	.326
ζ	0.020 \pm 0.007	0.021 \pm 0.008	0.018 \pm 0.008	.070

p Values from Wilcoxon signed-rank test between off-dAMPH ($n = 16$) and on-dAMPH ($n = 16$).

^a Significant p value.

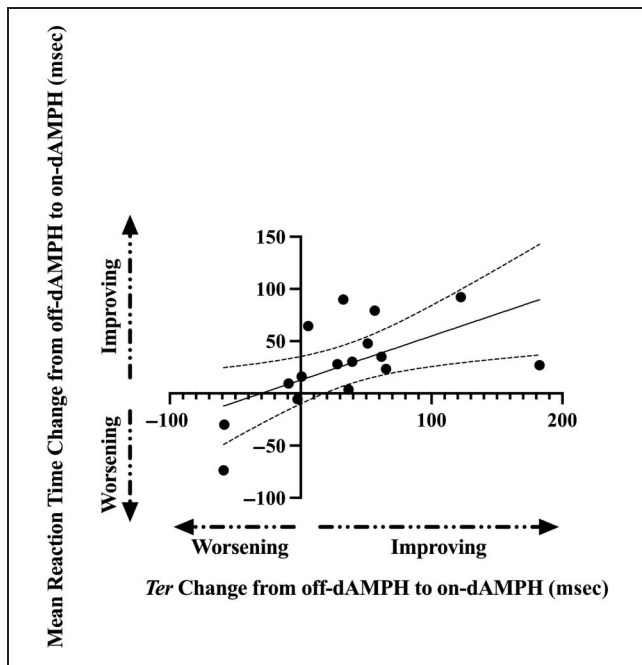


Figure 5. Scatterplot with line of best fit displaying the relationship between mean RT change (mean RT off-dAMPH – mean RT on-dAMPH) and *Ter* change (*Ter* off-dAMPH – *Ter* on-dAMPH). A GLM was applied with mean RT change as the dependent variable and change in DMC parameters as the independent variable. Age, sex, and MDS-UPDRS-III (off) scores served as covariates. A positive correlation between *Ter* change and mean RT change was observed ($p = .0205$).

Change in Mean Non-Decision Time Is Positively Correlated with Off-dAMPH [¹⁸F]fallypride BP_{ND} in the Globus Pallidus

We observed a positive correlation between off-dAMPH [¹⁸F]fallypride BP_{ND} in the globus pallidus and change in *Ter* (coefficient = 19.662, $p = .058$). This relationship

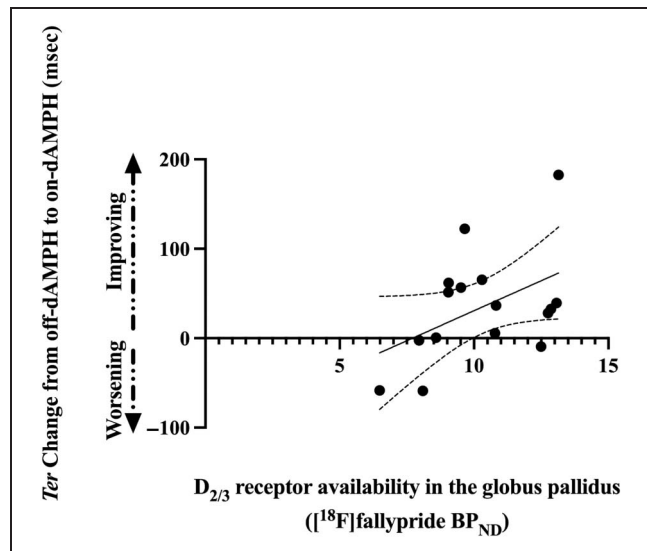


Figure 6. Scatterplot with line of best fit displaying the relationship between *Ter* change (*Ter* off-dAMPH – *Ter* on-dAMPH) and off-dAMPH [¹⁸F]fallypride BP_{ND}. A GLM was applied with change in DMC parameters as the dependent variable and mean ROI BP_{ND} as the independent variable. Age, sex, and MDS-UPDRS-III (off) scores served as covariates. A positive correlation between BP_{ND} in the globus pallidus and *Ter* change was observed ($p = .058$).

between off-dAMPH [¹⁸F]fallypride BP_{ND} in the globus pallidus and *Ter* change is shown in Figure 6. No significant correlations between off-dAMPH [¹⁸F]fallypride BP_{ND} and change in the other DMC parameters emerged. The results of the GLM analysis for all regions are presented in Table 4. We performed a corresponding analysis between change in DMC parameters and change in binding potential but did not observe any significant relationships.

Table 4. [¹⁸F]fallypride BP_{ND} (Off-dAMPH) Effects on Change in DMC Parameter *Ter*

ROI	Change in <i>Ter</i> ~ BP _{ND} + Age + Sex + UPDRS		
	95% CI	Coefficient	p^a (Adjusted p^b)
Ventral striatum	[-3.812, 28.535]	12.361	.121 (.182)
Caudate	[-6.081, 32.127]	13.023	.162 (.182)
Putamen	[-3.579, 20.025]	8.223	.153 (.182)
Substantia nigra	[-13.519, 227.474]	106.978	.077 (.172)
Globus pallidus	[6.773, 32.551]	19.662	.006 (.058)
Amygdala	[-4.507, 126.561]	61.027	.065 (.172)
Thalamus	[27.404, 335.414]	181.409	.025 (.113)
Hippocampus	[-105.530, 211.453]	52.961	.477 (.477)
Ventromedial OFC	[-6.389, 39.742]	16.676	.140 (.182)

GLM with FDR controlled at 0.05 to correct for multiple comparisons.

^a Uncorrected p value.

^b FDR-corrected p value.

Negative Relationship Between On-dAMPH Mean Non-Decision Time and [¹⁸F]fallypride BP_{ND} in the Basal Ganglia

Through an ROI-based analysis, we found a negative correlation between on-dAMPH *Ter* and on-dAMPH [¹⁸F]fallypride BP_{ND} in the putamen (coefficient = -15.919 , $p = .058$). A voxel-wise analysis confirmed this relationship in the right putamen (qFDR-corr < 0.01). This relationship matches the negative correlation identified between off-dAMPH *Ter* and off-dAMPH [¹⁸F]fallypride BP_{ND}.

DISCUSSION

This study examined the pathways underlying action control in patients with PD, dopamine release, and D₂-like receptor binding, by applying an evidence accumulation model to performance on the Simon conflict task. An analysis of DMC parameters and dopamine receptor availability across all participants demonstrated two dissociable relationships. First, an ROI-based analysis, which reflects average relations within a structurally defined a priori region, revealed a positive correlation in mesocorticolimbic regions, such that greater D₂-like BP_{ND} in the amygdala and ventromedial OFC is associated with longer non-decision time. Second, a voxel-based analysis, which captures effects that either occupy parts of a region or cut across regions, revealed a negative correlation in striatal and pallidal regions, such that greater D₂-like BP_{ND} in the putamen and globus pallidus is associated with shorter non-decision time.

The effect of dAMPH on Simon task performance established a beneficial role for the stimulant in reducing overall RT. The Simon effect estimates the impact of spatial interference and predicts that congruent trials will result in faster RTs. Accordingly, because this drug-induced improvement was similar in magnitude across congruent and incongruent conditions, dAMPH did not appear to regulate the Simon effect but rather facilitated overall RT. Within the DMC, a variation in mean non-decision time has a specific effect on model predictions as it changes mean RT in both congruent and incongruent conditions by the same amount. Thus, these results are consistent with a modulation of mean non-decision time by dAMPH in evidence accumulation models. This was further confirmed as the change in mean RT in response to dAMPH was positively correlated with the change in *Ter* in response to dAMPH, suggesting that dAMPH modulates non-decision processes upstream of the decision process, in the form of stimulus encoding, and/or downstream of the decision process, in the form of response output. Furthermore, investigating a change in *Ter* in relation to dopamine receptor availability disclosed a positive correlation in the globus pallidus, such that greater off-dAMPH D₂-like BP_{ND} is associated with faster non-decision time in response to dAMPH.

Limbic and Motor Loops

We interpret these results through the functional loop that connects mesial temporal areas to motor cortex for the purpose of supporting action control. Traditionally, cortico-basal ganglia-thalamocortical loops are thought to process limbic and sensorimotor information in parallel in closed, segregated systems (Alexander, DeLong, & Strick, 1986). However, it has long been proposed that the nucleus accumbens (ventral striatum) behaves as a limbic–motor interface by transforming limbic signals into motor output via pallidal and subcortical effector sites (Floresco, 2015; Mogenson, Jones, & Yim, 1980). More recently, findings from viral and optogenetic experiments with rodents suggest that the limbic and motor loops may be anatomically and functionally connected (Aoki et al., 2019). This interpretation is consistent with an open cortico-basal ganglia loop, whereby the ventral striatum projects to the substantia nigra pars reticulata and external globus pallidus, which subsequently sends input to the motor thalamus (Aoki et al., 2019). Our data demonstrate an example of this novel model, reflecting that limbic dopamine can regulate motor control. We show that dopaminergic receptor availability from limbic regions, especially the amygdala and ventromedial OFC, can modulate sensory and motor processing, likely through the nigropallidal network.

Novel Correlations Between Mesial Temporal Systems and Non-Decision Time in PD

This study is the first to analyze PET dopamine measurements to specifically examine Simon conflict task performance in persons with PD. fMRI scans with healthy humans have repeatedly identified the anterior and posterior cingulate, inferior temporal, inferior parietal, inferior frontal, dorsolateral prefrontal, supplementary motor, and visual association cortices, as well as the precuneus and caudate as areas relating to the Simon effect (Cespón, Hommel, Korsch, & Galashan, 2020; McIntosh & Sajda, 2020; Kerns, 2006; Liu, Banich, Jacobson, & Tanabe, 2004; Peterson et al., 2002). However, with an explicit focus on dopamine and PD, the amygdala, ventromedial OFC, insula, pallidum, and putamen manifested as the most meaningful regions for non-decision time in the Simon task.

Dopamine binding potential is a multifaceted measure whose interpretation relies on several factors. D_{2/3} receptors are expressed as autoreceptors on midbrain dopaminergic neurons in the ventral tegmental area and substantia nigra pars compacta, where they act presynaptically to decrease dopamine release (Ford, 2014; Missale, Nash, Robinson, Jaber, & Caron, 1998). Furthermore, D₂-like receptors are expressed on striatal medium spiny neurons, cortical pyramidal neurons, and mesolimbic pyramidal-like neurons and interneurons, where they act postsynaptically (Martel & Gatti McArthur, 2020;

Rosenkranz & Grace, 1999). In addition to the number of neurons and their intrinsic dopamine receptors, endogenous dopamine levels also impact dopamine binding potential values, as stimulants, such as methylphenidate or amphetamine, increase synaptic dopamine concentration and consequently decrease receptor availability measured with [^{18}F]fallypride (Laruelle et al., 1995, 1997; Volkow et al., 1994).

The positive relation between BP_{ND} in the amygdala and ventromedial OFC and non-decision time may reflect an impact of synaptic dopamine in these regions. As a measure of receptor availability, [^{18}F]fallypride BP_{ND} is increased if participants have less synaptic dopamine available and if there are more D_2 receptors, either because of trait differences or because of upregulation in response to lower dopamine levels. Although mesial temporal areas are subject to degeneration, this occurs to a lesser degree than for striatal regions, leaving limbic $\text{D}_{2/3}$ receptors relatively intact early in the disease process (Alberico, Cassell, & Narayanan, 2015; MacDonald & Monchi, 2011). However, there may nevertheless be some declines in synaptic dopamine leading to more available receptors, as well as some compensatory increases in $\text{D}_{2/3}$ receptors. Thus, the positive correlation between off-dAMPH BP_{ND} in mesial temporal regions and off-dAMPH non-decision latency may be capturing the beginning of a decrease in synaptic dopamine and the consequent lengthening of non-decision latency. Correspondingly, patients with greater synaptic dopamine availability in these regions demonstrate faster non-decision time.

Accordingly, the significant positive association between BP_{ND} and non-decision time highlights a noteworthy function of mesocorticolimbic regions for action control. Because this “emotional” system is not traditionally linked with the Simon conflict task, its apparent implication in action control in patients with PD suggests a compensatory mechanism. In line with theories of network degeneration, neural compensation may arise when changes in areas vital for specific behaviors require the activation of additional regions to carry out those behaviors (Barulli & Stern, 2013). Areas that are damaged later in the disease course and to a lesser degree may compensate for areas that are damaged earlier in the disease course and to a greater degree. Because of the relative preservation of mesial temporal areas, this system may offset the more pronounced degeneration of dorsal striatal areas, which traditionally participate in action control. These results are especially encouraging in terms of potential neuromodulatory targets. It is possible that neuromodulation, such as deep brain stimulation or TMS, that targets limbic regions could improve both motor performance and some non-motor measures, including memory and emotional regulation.

Moreover, these identified areas have been shown to contribute to processes inherent in the Simon conflict task, specifically non-decision steps. The correlations between non-decision time and dopamine receptors in the amygdala and OFC suggest a role in task-specific

stimulus detection and processing. Dopamine projections to the amygdala are recognized as regulators of associative learning. Although this mechanism characteristically concerns reward or aversion for fear conditioning and addiction, associative learning may also underlie advanced performance on the Simon task (Everitt et al., 1999; Maren & Fanselow, 1996). A participant’s ability to encode the relationship between stimulus color and the correct button choice, irrespective of stimulus location, likely improves over time and may be modulated by amygdalar dopamine. Moreover, the caudal medial OFC, recognized as a paralimbic cortical structure, has been linked to associations among flexible stimuli, responses, and outcomes (Elliott, Dolan, & Frith, 2000). As a correct response in the Simon task can be deemed “rewarding,” it is likely that dopaminergic signals in the ventromedial OFC assess and update the expected value of a response to a stimulus (Jenni, Li, & Floresco, 2021). Additionally, the paralimbic OFC may be important for regulating task state, comprising accumulated evidence about an action’s probable outcome in a given state (Stalnaker, Raheja, & Schoenbaum, 2021). Despite not reaching statistical significance, biologically pertinent clusters were also apparent in the locus coeruleus and substantia nigra. The failure to reach significance is likely due to the small sizes of these regions combined with the inherent constraints of PET imaging. Despite this limitation, the presence of these clusters is logical and encouraging, especially considering that monoamine release from the locus coeruleus to the hippocampus has been seen to enhance selective attention and spatial learning, prominent aspects of sensory processing in the Simon conflict task (Kempadoo, Mosharov, Choi, Sulzer, & Kandel, 2016). Because adeptness on the paradigm involves disregarding automatic processes, the ability to attend to the relevant feature of color and neglect the irrelevant feature of location is essential.

Basal Ganglia Dopamine and Sensory Motor Function

The negative voxel-wise association between D_2 -like BP_{ND} in the bilateral putamen, left globus pallidus, and right insular cortex and non-decision time is consistent with the effect of nigrostriatal dopamine loss on sensory and motor processing. We note that unlike D_2 -like BP_{ND} in mesial temporal areas, BP_{ND} in the putamen and globus pallidus may be indicative of dopamine degeneration because of the substantial involvement of the dorsal striatum early in PD. As such, the negative correlation between D_2 -like BP_{ND} in putaminal and pallidal regions and non-decision latency denotes the association between slower non-decision time and fewer $\text{D}_{2/3}$ receptors in these areas. Moreover, this negative relationship is maintained even when dAMPH is introduced, as less on-dAMPH [^{18}F]fallypride BP_{ND} is associated with greater on-dAMPH T_{er} . This interpretation is in line with evidence of differential dopaminergic cell loss along the dorsal-ventral axis, where reduced

[¹⁸F]dopa is most prominent in the dorsal putamen (Pavese & Brooks, 2009; Morrish, Sawle, & Brooks, 1995). The relationship with striatal BP_{ND} revealed in the voxel-wise regression adheres to this pattern (Figure 2). It is likely that reduced neuronal integrity in the putamen, which commonly regulates action control, motivates a reliance on mesial temporal regions.

Amphetamine Effects on Non-Decision Time as a Component of Action Control

It has long been speculated that dopamine is implicated in action control, especially given the effect of dopaminergic medications in persons with PD (Ruitenberget al., 2021; Mink, 1996). Several earlier studies exploring the intrinsic functions of action control support this hypothesis, reporting improved performance while participants were dosed with dopaminergic medication (Ruitenberget al., 2021; Costa et al., 2014). Investigations focusing specifically on the Simon conflict task in PD have likewise described a medication effect, whereby levodopa or dopamine agonist replacement therapy reduced the Simon effect on RT (Trujillo et al., 2019; van Wouwe et al., 2016). In lieu of comparing performance on and off dopaminergic medication, we implemented an amphetamine challenge to measure stimulated dopamine release and assess this index of dopamine system reactivity (Riccardi et al., 2006). Interestingly, with this method, a unique picture emerges as dAMPH speeds up RT but does not alter the Simon effect. Therefore, dAMPH, which increases catecholamine levels in the synaptic cleft, appears to accomplish its reduction of RT by impacting non-decisional processes rather than decisional processes (Heal, Smith, Gosden, & Nutt, 2013).

The finding of dAMPH's preferential interaction with non-decision latency aligns with previous work in both healthy adults and rats and Parkinsonian animal models. Research consistently shows that psychostimulants induce motor activation (Swerdlow, Vaccarino, Amalric, & Koob, 1986). This effect is noted in humans administered dAMPH, with reports of augmented locomotion through increased spontaneous motor activity and increased acceleration (Minassian et al., 2016; Greenwald et al., 1998). Moreover, the standard amphetamine-induced rotation test aptly demonstrates the role of the drug in recovering motor function for 6-OHDA lesion models (Björklund & Dunnett, 2019; Ungerstedt & Arbuthnott, 1970). However, in addition to contributing to motor behavior, amphetamine also influences sensory mechanisms. Further investigations into the stimulant in healthy humans have shown enhanced information processing with dAMPH and facilitation of sensory processing with methamphetamine (Van Hedger, Keedy, Schertz, Berman, & de Wit, 2019; Fillmore, Kelly, & Martin, 2005). As our results highlight *Ter*, they pinpoint sensory processing and motor execution as the key players in dAMPH's advantageous effect on RT.

Dopamine and the Limbic–Motor Network

The effect of dAMPH on change in Simon conflict task performance is restricted to the pallidum, with greater off-dAMPH D₂-like BP_{ND} in the globus pallidus associated with more positive *Ter* change (better performance with dAMPH). We see that patients with higher off-dAMPH BP_{ND} in the globus pallidus benefit the most from dAMPH-induced dopamine release. This improvement may be associated with increased nigral dopaminergic input that may subsequently activate pallidal effector sites for motor output. These results do not directly demonstrate functional connectivity with the pallidum. However, recent tracing work has proposed that the rat dorsomedial striatum, likely homologous to the human globus pallidus, projects to the medial substantia nigra pars reticulata and can subsequently target motor thalamus (Aoki et al., 2019). Additionally, connectivity studies have shown metabolic relationships among the globus pallidus, SMA, amygdala, and other regions in patients with PD (Vo et al., 2023). Accordingly, our findings of (1) a positive relationship between binding potential in mesolimbic regions and off-dAMPH task performance and (2) a positive relationship between binding potential in the pallidum and dAMPH-driven task improvement suggest that signals emerging from the amygdala and OFC may project through the globus pallidus to generate motor output.

Conclusions and Limitations

Despite the notable dAMPH-induced reduction of non-decision time, by evaluating Simon conflict task performance 30 min after dAMPH exposure, it is possible that we may not have measured the full impact of increased dopamine. Enforcing a longer delay of approximately 2 hr between drug administration and cognitive testing may have resulted in a larger dAMPH effect in the globus pallidus and novel effects in mesocorticolimbic regions (Fillmore et al., 2005). Moreover, although we claim that these findings are due to dopaminergic activity, it is important to note that dAMPH also secondarily interacts with other neurotransmitters, including acetylcholine, serotonin, and norepinephrine (Moore, 1977). We acknowledge the limitations of a small sample size for the dAMPH challenge and are hopeful that future studies with an increased number of patients will further corroborate these findings. Finally, we recognize that the results do not establish functional connectivity between limbic regions and the globus pallidus for motor output but are optimistic that novel stereoelectroencephalography methods will allow us to study causal and functional relationships between these areas.

Although this study addresses PD exclusively, the results have importance to other clinical conditions that impact action control. The findings further support investigations in other Parkinsonian disorders that present with

impulsivity and may have greater limbic pathology, including PSP and frontotemporal dementia. Additionally, the implication of a translational limbic–motor interface, with mesial temporal and globus pallidal activity, provides a compelling demonstration of the rich interactions between limbic processing and motor behavior. Connections between movement and psychological factors have frequently been cited as an explanation for motor disorders linked to emotional dysregulation. Accordingly, motor conversion disorder and the analogous psychogenic movement disorder are associated with comorbid psychiatric disorders, including anxiety and depression, and adverse life events (Kranick et al., 2011; Roelofs, Spinhoven, Sandijck, Moene, & Hoogduin, 2005; Sar, Akyüz, Kundakçi, Kiziltan, & Dogan, 2004). Evidence suggestive of this intermingled relationship between the limbic and motor systems consists of increased amygdala activation, enhanced functional connectivity between the motor cortex and posterior cingulate cortex, and greater functional connectivity between the amygdala and SMA (Aybek et al., 2015; Voon et al., 2010; Cojan, Waber, Carruzzo, & Vuilleumier, 2009). However, translational evidence of the correlation between the two has remained tenuous. The results of the current study strengthen the claim of a functional limbic–motor loop by demonstrating mesocorticolimbic and pallidal dopaminergic influence over motor behavior.

Reprint requests should be sent to Daniel O. Claassen, Department of Neurology, Vanderbilt University Medical Center, Nashville, TN 37232, or via e-mail: daniel.claassen@vumc.org.

Data Availability Statement

All data reported in this article will be shared by the lead contact upon request. Any additional information required to reanalyze the data reported in this article is also available from the lead contact upon request.

Author Contributions

Leah G. Mann: Formal analysis; Software; Visualization; Writing—Original draft; Writing—Review & editing. Mathieu Servant: Formal analysis; Methodology; Software; Visualization; Writing—Review & editing. Kaitlyn R. Hay: Data curation; Investigation; Resources. Alexander K. Song: Data curation; Formal analysis; Investigation; Writing—Review & editing. Paula Trujillo: Data curation; Investigation; Writing—Review & editing. Bailu Yan: Formal analysis. Hakmook Kang: Formal analysis; Writing—Review & editing. David Zald: Conceptualization; Methodology; Writing—Review & editing. Manus J. Donahue: Methodology. Gordon D. Logan: Formal analysis; Writing—Review & editing. Daniel Claassen: Conceptualization; Funding acquisition; Methodology; Supervision; Writing—Review & editing.

Funding Information

Daniel O. Claassen, National Institute on Aging (<https://dx.doi.org/10.13039/100000049>), grant number: 1K24AG064114. Daniel O. Claassen, National Institute of Neurological Disorders and Stroke (<https://dx.doi.org/10.13039/100000065>), grant number: 5R01NS097783.

Diversity in Citation Practices

Retrospective analysis of the citations in every article published in this journal from 2010 to 2021 reveals a persistent pattern of gender imbalance: Although the proportions of authorship teams (categorized by estimated gender identification of first author/last author) publishing in the *Journal of Cognitive Neuroscience (JoCN)* during this period were $M(\text{an})/M = .407$, $W(\text{oman})/M = .32$, $M/W = .115$, and $W/W = .159$, the comparable proportions for the articles that these authorship teams cited were $M/M = .549$, $W/M = .257$, $M/W = .109$, and $W/W = .085$ (Postle and Fulvio, *JoCN*, 34:1, pp. 1–3). Consequently, *JoCN* encourages all authors to consider gender balance explicitly when selecting which articles to cite and gives them the opportunity to report their article’s gender citation balance. The authors of this paper report its proportions of citations by gender category to be: $M/M = .553$; $W/M = .276$; $M/W = .105$; $W/W = .066$.

REFERENCES

- Ahlskog, J. E. (2011). Pathological behaviors provoked by dopamine agonist therapy of Parkinson’s disease. *Physiology & Behavior*, 104, 168–172. <https://doi.org/10.1016/j.physbeh.2011.04.055>, PubMed: 21557955
- Alberico, S. L., Cassell, M. D., & Narayanan, N. S. (2015). The vulnerable ventral tegmental area in Parkinson’s disease. *Basal Ganglia*, 5, 51–55. <https://doi.org/10.1016/j.baga.2015.06.001>, PubMed: 26251824
- Albrecht, D. S., Kareken, D. A., Christian, B. T., Dziedzic, M., & Yoder, K. K. (2014). Cortical dopamine release during a behavioral response inhibition task. *Synapse*, 68, 266–274. <https://doi.org/10.1002/syn.21736>, PubMed: 24677429
- Alexander, G. E., DeLong, M. R., & Strick, P. L. (1986). Parallel organization of functionally segregated circuits linking basal ganglia and cortex. *Annual Review of Neuroscience*, 9, 357–381. <https://doi.org/10.1146/annurev.ne.09.030186.002041>, PubMed: 3085570
- Amiri, S., Arbabi, M., Rahimi, M., Badragheh, F., Zibadi, H. A., Asadi-Pooya, A. A., et al. (2021). Effective connectivity between emotional and motor brain regions in people with psychogenic nonepileptic seizures (PNES). *Epilepsy & Behavior*, 122, 108085. <https://doi.org/10.1016/j.yebeh.2021.108085>, PubMed: 34166951
- Aoki, S., Smith, J. B., Li, H., Yan, X., Igarashi, M., Coulon, P., et al. (2019). An open cortico-basal ganglia loop allows limbic control over motor output via the nigrothalamic pathway. *eLife*, 8, e49995. <https://doi.org/10.7554/eLife.49995>, PubMed: 31490123
- Aybek, S., Nicholson, T. R., O’Daly, O., Zelaya, F., Kanaan, R. A., & David, A. S. (2015). Emotion–motion interactions in conversion disorder: An fMRI study. *PLoS One*, 10, e0123273.

- <https://doi.org/10.1371/journal.pone.0123273>, PubMed: 25859660
- Barulli, D., & Stern, Y. (2013). Efficiency, capacity, compensation, maintenance, plasticity: Emerging concepts in cognitive reserve. *Trends in Cognitive Sciences*, *17*, 502–509. <https://doi.org/10.1016/j.tics.2013.08.012>, PubMed: 24018144
- Benjamini, Y., & Hochberg, Y. (1995). Controlling the false discovery rate: A practical and powerful approach to multiple testing. *Journal of the Royal Statistical Society: Series B (Methodological)*, *57*, 289–300. <https://doi.org/10.1111/j.2517-6161.1995.tb02031.x>
- Björklund, A., & Dunnett, S. B. (2019). The amphetamine induced rotation test: A re-assessment of its use as a tool to monitor motor impairment and functional recovery in rodent models of Parkinson's disease. *Journal of Parkinson's Disease*, *9*, 17–29. <https://doi.org/10.3233/JPD-181525>, PubMed: 30741691
- Buckholz, J. W., Treadway, M. T., Cowan, R. L., Woodward, N. D., Li, R., Ansari, M. S., et al. (2010). Dopaminergic network differences in human impulsivity. *Science*, *329*, 532. <https://doi.org/10.1126/science.1185778>, PubMed: 20671181
- Camps, M., Cortés, R., Gueye, B., Probst, A., & Palacios, J. M. (1989). Dopamine receptors in human brain: Autoradiographic distribution of D2 sites. *Neuroscience*, *28*, 275–290. [https://doi.org/10.1016/0306-4522\(89\)90179-6](https://doi.org/10.1016/0306-4522(89)90179-6), PubMed: 2522167
- Cespón, J., Hommel, B., Korsch, M., & Galashan, D. (2020). The neurocognitive underpinnings of the Simon effect: An integrative review of current research. *Cognitive, Affective, & Behavioral Neuroscience*, *20*, 1133–1172. <https://doi.org/10.3758/s13415-020-00836-y>, PubMed: 33025513
- Claassen, D. O., Stark, A. J., Spears, C. A., Petersen, K. J., van Wouwe, N. C., Kessler, R. M., et al. (2017). Mesocorticolimbic hemodynamic response in Parkinson's disease patients with compulsive behaviors. *Movement Disorders*, *32*, 1574–1583. <https://doi.org/10.1002/mds.27047>, PubMed: 28627133
- Claassen, D. O., van den Wildenberg, W. P., Harrison, M. B., van Wouwe, N. C., Kanoff, K., Neimat, J. S., et al. (2015). Proficient motor impulse control in Parkinson disease patients with impulsive and compulsive behaviors. *Pharmacology, Biochemistry, and Behavior*, *129*, 19–25. <https://doi.org/10.1016/j.pbb.2014.11.017>, PubMed: 25459105
- Cojan, Y., Waber, L., Carruzzo, A., & Vuilleumier, P. (2009). Motor inhibition in hysterical conversion paralysis. *Neuroimage*, *47*, 1026–1037. <https://doi.org/10.1016/j.neuroimage.2009.05.023>, PubMed: 19450695
- Costa, A., Peppe, A., Mazzù, I., Longarzo, M., Caltagirone, C., & Carlesimo, G. A. (2014). Dopamine treatment and cognitive functioning in individuals with Parkinson's disease: The “cognitive flexibility” hypothesis seems to work. *Behavioural Neurology*, *2014*, 260896. <https://doi.org/10.1155/2014/260896>, PubMed: 24825952
- De Jong, R., Liang, C. C., & Lauber, E. (1994). Conditional and unconditional automaticity: A dual-process model of effects of spatial stimulus-response correspondence. *Journal of Experimental Psychology: Human Perception and Performance*, *20*, 731–750. <https://doi.org/10.1037/0096-1523.20.4.731>, PubMed: 8083631
- Elliott, R., Dolan, R. J., & Frith, C. D. (2000). Dissociable functions in the medial and lateral orbitofrontal cortex: Evidence from human neuroimaging studies. *Cerebral Cortex*, *10*, 308–317. <https://doi.org/10.1093/cercor/10.3.308>, PubMed: 10731225
- Ersche, K. D., Roiser, J. P., Abbott, S., Craig, K. J., Müller, U., Suckling, J., et al. (2011). Response perseveration in stimulant dependence is associated with striatal dysfunction and can be ameliorated by a D2/3 receptor agonist. *Biological Psychiatry*, *70*, 754–762. <https://doi.org/10.1016/j.biopsych.2011.06.033>, PubMed: 21967987
- Everitt, B. J., Parkinson, J. A., Olmstead, M. C., Arroyo, M., Robledo, P., & Robbins, T. W. (1999). Associative processes in addiction and reward. The role of amygdala-ventral striatal subsystems. *Annals of the New York Academy of Sciences*, *877*, 412–438. <https://doi.org/10.1111/j.1749-6632.1999.tb09280.x>, PubMed: 10415662
- Fabbri, G., Juncos, J., Mouradian, M. M., Serrati, C., & Chase, T. N. (1987). Levodopa pharmacokinetic mechanisms and motor fluctuations in Parkinson's disease. *Annals of Neurology*, *21*, 370–376. <https://doi.org/10.1002/ana.410210409>, PubMed: 3579222
- Fillmore, M. T., Kelly, T. H., & Martin, C. A. (2005). Effects of d-amphetamine in human models of information processing and inhibitory control. *Drug and Alcohol Dependence*, *77*, 151–159. <https://doi.org/10.1016/j.drugalcdep.2004.07.013>, PubMed: 15664716
- Floresco, S. B. (2015). The nucleus accumbens: An interface between cognition, emotion, and action. *Annual Review of Psychology*, *66*, 25–52. <https://doi.org/10.1146/annurev-psych-010213-115159>, PubMed: 25251489
- Ford, C. P. (2014). The role of D2-autoreceptors in regulating dopamine neuron activity and transmission. *Neuroscience*, *282*, 13–22. <https://doi.org/10.1016/j.neuroscience.2014.01.025>, PubMed: 24463000
- Ghahremani, D. G., Lee, B., Robertson, C. L., Tabibnia, G., Morgan, A. T., De Shetler, N., et al. (2012). Striatal dopamine D₂/D₃ receptors mediate response inhibition and related activity in frontostriatal neural circuitry in humans. *Journal of Neuroscience*, *32*, 7316–7324. <https://doi.org/10.1523/JNEUROSCI.4284-11.2012>, PubMed: 22623677
- Goetz, C. G., Tilley, B. C., Shaftman, S. R., Stebbins, G. T., Fahn, S., Martinez-Martin, P., et al. (2008). Movement Disorder Society-sponsored revision of the Unified Parkinson's Disease Rating Scale (MDS-UPDRS): Scale presentation and clinimetric testing results. *Movement Disorders*, *23*, 2129–2170. <https://doi.org/10.1002/mds.22340>, PubMed: 19025984
- Greenwald, M. K., Schuster, C. R., Johanson, C. E., & Jewell, J. (1998). Automated measurement of motor activity in human subjects: Effects of repeated testing and d-amphetamine. *Pharmacology, Biochemistry, and Behavior*, *59*, 59–65. [https://doi.org/10.1016/S0091-3057\(97\)00387-0](https://doi.org/10.1016/S0091-3057(97)00387-0), PubMed: 9443537
- Heal, D. J., Smith, S. L., Gosden, J., & Nutt, D. J. (2013). Amphetamine, past and present—A pharmacological and clinical perspective. *Journal of Psychopharmacology*, *27*, 479–496. <https://doi.org/10.1177/0269881113482532>, PubMed: 23539642
- Heitz, R. P. (2014). The speed-accuracy tradeoff: History, physiology, methodology, and behavior. *Frontiers in Neuroscience*, *8*, 150. <https://doi.org/10.3389/fnins.2014.00150>, PubMed: 24966810
- Hommel, B. (1994). Spontaneous decay of response-code activation. *Psychological Research*, *56*, 261–268. <https://doi.org/10.1007/BF00419656>, PubMed: 8090861
- Hughes, A. J., Daniel, S. E., Kilford, L., & Lees, A. J. (1992). Accuracy of clinical diagnosis of idiopathic Parkinson's disease: A clinico-pathological study of 100 cases. *Journal of Neurology, Neurosurgery, and Psychiatry*, *55*, 181–184. <https://doi.org/10.1136/jnnp.55.3.181>, PubMed: 1564476
- Jenni, N. L., Li, Y. T., & Floresco, S. B. (2021). Medial orbitofrontal cortex dopamine D₁/D₂ receptors differentially modulate distinct forms of probabilistic decision-making. *Neuropsychopharmacology*, *46*, 1240–1251. <https://doi.org/10.1038/s41386-020-00931-1>, PubMed: 33452435

- Jentsch, J. D., & Pennington, Z. T. (2014). Reward, interrupted: Inhibitory control and its relevance to addictions. *Neuropharmacology*, *76*, 479–486. <https://doi.org/10.1016/j.neuropharm.2013.05.022>, PubMed: 23748054
- Kempadoo, K. A., Mosharov, E. V., Choi, S. J., Sulzer, D., & Kandel, E. R. (2016). Dopamine release from the locus coeruleus to the dorsal hippocampus promotes spatial learning and memory. *Proceedings of the National Academy of Sciences, U.S.A.*, *113*, 14835–14840. <https://doi.org/10.1073/pnas.1616515114>, PubMed: 27930324
- Kerns, J. G. (2006). Anterior cingulate and prefrontal cortex activity in an fMRI study of trial-to-trial adjustments on the Simon task. *Neuroimage*, *33*, 399–405. <https://doi.org/10.1016/j.neuroimage.2006.06.012>, PubMed: 16876434
- Koelega, H. S. (1993). Stimulant drugs and vigilance performance: A review. *Psychopharmacology*, *111*, 1–16. <https://doi.org/10.1007/BF02257400>, PubMed: 7870923
- Kranick, S., Ekanayake, V., Martinez, V., Ameli, R., Hallett, M., & Voon, V. (2011). Psychopathology and psychogenic movement disorders. *Movement Disorders*, *26*, 1844–1850. <https://doi.org/10.1002/mds.23830>, PubMed: 21714007
- Laruelle, M., Abi-Dargham, A., van Dyck, C. H., Rosenblatt, W., Zea-Ponce, Y., Zoghbi, S. S., et al. (1995). SPECT imaging of striatal dopamine release after amphetamine challenge. *Journal of Nuclear Medicine*, *36*, 1182–1190. PubMed: 7790942
- Laruelle, M., D'Souza, C. D., Baldwin, R. M., Abi-Dargham, A., Kanes, S. J., Fingado, C. L., et al. (1997). Imaging D2 receptor occupancy by endogenous dopamine in humans. *Neuropsychopharmacology*, *17*, 162–174. [https://doi.org/10.1016/S0893-133X\(97\)00043-2](https://doi.org/10.1016/S0893-133X(97)00043-2), PubMed: 9272483
- Liu, X., Banich, M. T., Jacobson, B. L., & Tanabe, J. L. (2004). Common and distinct neural substrates of attentional control in an integrated Simon and spatial Stroop task as assessed by event-related fMRI. *Neuroimage*, *22*, 1097–1106. <https://doi.org/10.1016/j.neuroimage.2004.02.033>, PubMed: 15219581
- Logan, G. D. (1988). Toward an instance theory of automatization. *Psychological Review*, *95*, 492–527. <https://doi.org/10.1037/0033-295X.95.4.492>
- Macdonald, P. A., & Monchi, O. (2011). Differential effects of dopaminergic therapies on dorsal and ventral striatum in Parkinson's disease: Implications for cognitive function. *Parkinson's Disease*, *2011*, 572743. <https://doi.org/10.4061/2011/572743>, PubMed: 21437185
- Mackey, S., & Petrides, M. (2009). Architectonic mapping of the medial region of the human orbitofrontal cortex by density profiles. *Neuroscience*, *159*, 1089–1107. <https://doi.org/10.1016/j.neuroscience.2009.01.036>, PubMed: 19356690
- Mann, L. G., Hay, K. R., Song, A. K., Errington, S. P., Trujillo, P., Zald, D. H., et al. (2021). D₂-like receptor expression in the hippocampus and amygdala informs performance on the stop-signal task in Parkinson's disease. *Journal of Neuroscience*, *41*, 10023–10030. <https://doi.org/10.1523/JNEUROSCI.0968-21.2021>, PubMed: 34750225
- Maren, S., & Fanselow, M. S. (1996). The amygdala and fear conditioning: has the nut been cracked? *Neuron*, *16*, 237–240. [https://doi.org/10.1016/S0896-6273\(00\)80041-0](https://doi.org/10.1016/S0896-6273(00)80041-0), PubMed: 8789938
- Martel, J. C., & Gatti McArthur, S. (2020). Dopamine receptor subtypes, physiology and pharmacology: New ligands and concepts in schizophrenia. *Frontiers in Pharmacology*, *11*, 1003. <https://doi.org/10.3389/fphar.2020.01003>, PubMed: 32765257
- Mayfield, R. D., Randall, P. K., Spirduso, W. W., & Wilcox, R. E. (1993). Apomorphine and amphetamine produce differential effects on the speed and success of reaction time responding in the rat. *Pharmacology, Biochemistry, and Behavior*, *46*, 769–775. [https://doi.org/10.1016/0091-3057\(93\)90199-4](https://doi.org/10.1016/0091-3057(93)90199-4), PubMed: 8309953
- McIntosh, J. R., & Sajda, P. (2020). Decomposing Simon task BOLD activation using a drift-diffusion model framework. *Scientific Reports*, *10*, 3938. <https://doi.org/10.1038/s41598-020-60943-1>, PubMed: 32127617
- Minassian, A., Young, J. W., Cope, Z. A., Henry, B. L., Geyer, M. A., & Perry, W. (2016). Amphetamine increases activity but not exploration in humans and mice. *Psychopharmacology*, *233*, 225–233. <https://doi.org/10.1007/s00213-015-4098-4>, PubMed: 26449721
- Mink, J. W. (1996). The basal ganglia: Focused selection and inhibition of competing motor programs. *Progress in Neurobiology*, *50*, 381–425. [https://doi.org/10.1016/S0301-0082\(96\)00042-1](https://doi.org/10.1016/S0301-0082(96)00042-1), PubMed: 9004351
- Missale, C., Nash, S. R., Robinson, S. W., Jaber, M., & Caron, M. G. (1998). Dopamine receptors: From structure to function. *Physiological Reviews*, *78*, 189–225. <https://doi.org/10.1152/physrev.1998.78.1.189>, PubMed: 9457173
- Moeller, F. G., Barratt, E. S., Dougherty, D. M., Schmitz, J. M., & Swann, A. C. (2001). Psychiatric aspects of impulsivity. *American Journal of Psychiatry*, *158*, 1783–1793. <https://doi.org/10.1176/appi.ajp.158.11.1783>, PubMed: 11691682
- Mogenson, G. J., Jones, D. L., & Yim, C. Y. (1980). From motivation to action: Functional interface between the limbic system and the motor system. *Progress in Neurobiology*, *14*, 69–97. [https://doi.org/10.1016/0301-0082\(80\)90018-0](https://doi.org/10.1016/0301-0082(80)90018-0), PubMed: 6999537
- Moore, K. E. (1977). The actions of amphetamine on neurotransmitters: A brief review. *Biological Psychiatry*, *12*, 451–462. PubMed: 17437
- Morrish, P. K., Sawle, G. V., & Brooks, D. J. (1995). Clinical and [18F] dopa PET findings in early Parkinson's disease. *Journal of Neurology, Neurosurgery, and Psychiatry*, *59*, 597–600. <https://doi.org/10.1136/jnnp.59.6.597>, PubMed: 7500096
- Mukherjee, J., Christian, B. T., Dunigan, K. A., Shi, B., Narayanan, T. K., Satter, M., et al. (2002). Brain imaging of 18F-fallypride in normal volunteers: Blood analysis, distribution, test-retest studies, and preliminary assessment of sensitivity to aging effects on dopamine D-2/D-3 receptors. *Synapse*, *46*, 170–188. <https://doi.org/10.1002/syn.10128>, PubMed: 12325044
- Pavese, N., & Brooks, D. J. (2009). Imaging neurodegeneration in Parkinson's disease. *Biochimica et Biophysica Acta*, *1792*, 722–729. <https://doi.org/10.1016/j.bbadis.2008.10.003>, PubMed: 18992326
- Petersen, K., Van Wouwe, N., Stark, A., Lin, Y. C., Kang, H., Trujillo-Diaz, P., et al. (2018). Ventral striatal network connectivity reflects reward learning and behavior in patients with Parkinson's disease. *Human Brain Mapping*, *39*, 509–521. <https://doi.org/10.1002/hbm.23860>, PubMed: 29086460
- Peterson, B. S., Kane, M. J., Alexander, G. M., Lacadie, C., Skudlarski, P., Leung, H. C., et al. (2002). An event-related functional MRI study comparing interference effects in the Simon and Stroop tasks. *Cognitive Brain Research*, *13*, 427–440. [https://doi.org/10.1016/S0926-6410\(02\)00054-X](https://doi.org/10.1016/S0926-6410(02)00054-X), PubMed: 11919006
- Pohjalainen, T., Rinne, J. O., Någren, K., Syvälahti, E., & Hietala, J. (1998). Sex differences in the striatal dopamine D2 receptor binding characteristics in vivo. *American Journal of Psychiatry*, *155*, 768–773. <https://doi.org/10.1176/ajp.155.6.768>, PubMed: 9619148
- Ratcliff, R., & McKoon, G. (2008). The diffusion decision model: Theory and data for two-choice decision tasks. *Neural Computation*, *20*, 873–922. <https://doi.org/10.1162/neco.2008.12.06.420>, PubMed: 18085991

- Ratcliff, R., Smith, P. L., Brown, S. D., & McKoon, G. (2016). Diffusion decision model: Current issues and history. *Trends in Cognitive Sciences*, *20*, 260–281. <https://doi.org/10.1016/j.tics.2016.01.007>, PubMed: 26952739
- Riccardi, P., Li, R., Ansari, M. S., Zald, D., Park, S., Dawant, B., et al. (2006). Amphetamine-induced displacement of [^{18}F] fallypride in striatum and extrastriatal regions in humans. *Neuropsychopharmacology*, *31*, 1016–1026. <https://doi.org/10.1038/sj.npp.1300916>, PubMed: 16237395
- Ridderinkhof, K. R. (2002). Activation and suppression in conflict tasks: Empirical clarification through distributional analyses. In W. Prinz & B. Hommel (Eds.), *Mechanisms in perception and action, attention and performance XIX* (pp. 494–519). Oxford: Oxford University Press.
- Roelofs, K., Spinhoven, P., Sandijck, P., Moene, F. C., & Hoogduin, K. A. (2005). The impact of early trauma and recent life-events on symptom severity in patients with conversion disorder. *Journal of Nervous and Mental Disease*, *193*, 508–514. <https://doi.org/10.1097/01.nmd.0000172472.60197.4d>, PubMed: 16082294
- Rosenkranz, J. A., & Grace, A. A. (1999). Modulation of basolateral amygdala neuronal firing and afferent drive by dopamine receptor activation in vivo. *Journal of Neuroscience*, *19*, 11027–11039. <https://doi.org/10.1523/JNEUROSCI.19-24-11027.1999>, PubMed: 10594083
- Ruitenbergh, M. F. L., van Wouwe, N. C., Wylie, S. A., & Abrahamse, E. L. (2021). The role of dopamine in action control: Insights from medication effects in Parkinson's disease. *Neuroscience and Biobehavioral Reviews*, *127*, 158–170. <https://doi.org/10.1016/j.neubiorev.2021.04.023>, PubMed: 33905788
- Sar, V., Akyüz, G., Kundakçi, T., Kiziltan, E., & Dogan, O. (2004). Childhood trauma, dissociation, and psychiatric comorbidity in patients with conversion disorder. *American Journal of Psychiatry*, *161*, 2271–2276. <https://doi.org/10.1176/ajp.161.12.2271>, PubMed: 15569899
- Servant, M., van Wouwe, N., Wylie, S. A., & Logan, G. D. (2018). A model-based quantification of action control deficits in Parkinson's disease. *Neuropsychologia*, *111*, 26–35. <https://doi.org/10.1016/j.neuropsychologia.2018.01.014>, PubMed: 29360609
- Simon, J. R. (1969). Reactions toward the source of stimulation. *Journal of Experimental Psychology*, *81*, 174–176. <https://doi.org/10.1037/h0027448>, PubMed: 5812172
- Simon, J. R., & Rudell, A. P. (1967). Auditory S-R compatibility: The effect of an irrelevant cue on information processing. *Journal of Applied Psychology*, *51*, 300–304. <https://doi.org/10.1037/h0020586>, PubMed: 6045637
- Skinbjerg, M., Liow, J. S., Seneca, N., Hong, J., Lu, S., Thorsell, A., et al. (2010). D2 dopamine receptor internalization prolongs the decrease of radioligand binding after amphetamine: A PET study in a receptor internalization-deficient mouse model. *Neuroimage*, *50*, 1402–1407. <https://doi.org/10.1016/j.neuroimage.2010.01.055>, PubMed: 20097293
- Song, A. K., Hay, K. R., Trujillo, P., Aumann, M., Stark, A. J., Yan, Y., et al. (2022). Amphetamine-induced dopamine release and impulsivity in Parkinson's disease. *Brain*, *145*, 3488–3499. <https://doi.org/10.1093/brain/awab487>, PubMed: 34951464
- Stalnaker, T. A., Raheja, N., & Schoenbaum, G. (2021). Orbitofrontal state representations are related to choice adaptations and reward predictions. *Journal of Neuroscience*, *41*, 1941–1951. <https://doi.org/10.1523/JNEUROSCI.0753-20.2020>, PubMed: 33446521
- Stark, A. J., Smith, C. T., Lin, Y. C., Petersen, K. J., Trujillo, P., van Wouwe, N. C., et al. (2018). Nigrostriatal and mesolimbic D_{2/3} receptor expression in Parkinson's disease patients with compulsive reward-driven behaviors. *Journal of Neuroscience*, *38*, 3230–3239. <https://doi.org/10.1523/JNEUROSCI.3082-17.2018>, PubMed: 29483278
- Stark, A. J., Smith, C. T., Petersen, K. J., Trujillo, P., van Wouwe, N. C., Donahue, M. J., et al. (2018). [^{18}F]fallypride characterization of striatal and extrastriatal D_{2/3} receptors in Parkinson's disease. *NeuroImage: Clinical*, *18*, 433–442. <https://doi.org/10.1016/j.nicl.2018.02.010>, PubMed: 29541577
- Steeves, T. D., Miyasaki, J., Zurowski, M., Lang, A. E., Pellecchia, G., Van Eimeren, T., et al. (2009). Increased striatal dopamine release in Parkinsonian patients with pathological gambling: A [^{11}C] raclopride PET study. *Brain*, *132*, 1376–1385. <https://doi.org/10.1093/brain/awp054>, PubMed: 19346328
- Swerdlow, N. R., Vaccarino, F. J., Amalric, M., & Koob, G. F. (1986). The neural substrates for the motor-activating properties of psychostimulants: A review of recent findings. *Pharmacology, Biochemistry, and Behavior*, *25*, 233–248. [https://doi.org/10.1016/0091-3057\(86\)90261-3](https://doi.org/10.1016/0091-3057(86)90261-3), PubMed: 2875470
- Tomlinson, C. L., Stowe, R., Patel, S., Rick, C., Gray, R., & Clarke, C. E. (2010). Systematic review of levodopa dose equivalency reporting in Parkinson's disease. *Movement Disorders*, *25*, 2649–2653. <https://doi.org/10.1002/mds.23429>, PubMed: 21069833
- Tompson, D., & Oliver-Willwong, R. (2009). Pharmacokinetic and pharmacodynamic comparison of ropinirole 24-hour prolonged release and ropinirole immediate release in patients with Parkinson's disease. *Clinical Neuropharmacology*, *32*, 140–148. <https://doi.org/10.1097/WNF.0b013e318176c505>, PubMed: 18978485
- Trujillo, P., van Wouwe, N. C., Lin, Y. C., Stark, A. J., Petersen, K. J., Kang, H., et al. (2019). Dopamine effects on frontal cortical blood flow and motor inhibition in Parkinson's disease. *Cortex*, *115*, 99–111. <https://doi.org/10.1016/j.cortex.2019.01.016>, PubMed: 30776736
- Ulrich, R., Schröter, H., Leuthold, H., & Birngruber, T. (2015). Automatic and controlled stimulus processing in conflict tasks: Superimposed diffusion processes and delta functions. *Cognitive Psychology*, *78*, 148–174. <https://doi.org/10.1016/j.cogpsych.2015.02.005>, PubMed: 25909766
- Ungerstedt, U., & Arbuthnott, G. W. (1970). Quantitative recording of rotational behavior in rats after 6-hydroxy-dopamine lesions of the nigrostriatal dopamine system. *Brain Research*, *24*, 485–493. [https://doi.org/10.1016/0006-8993\(70\)90187-3](https://doi.org/10.1016/0006-8993(70)90187-3), PubMed: 5494536
- van der Kruijs, S. J., Bodde, N. M., Vaessen, M. J., Lazeron, R. H., Vonck, K., Boon, P., et al. (2012). Functional connectivity of dissociation in patients with psychogenic non-epileptic seizures. *Journal of Neurology, Neurosurgery, and Psychiatry*, *83*, 239–247. <https://doi.org/10.1136/jnnp-2011-300776>, PubMed: 22056967
- Van Hedger, K., Keedy, S. K., Schertz, K. E., Berman, M. G., & de Wit, H. (2019). Effects of methamphetamine on neural responses to visual stimuli. *Psychopharmacology*, *236*, 1741–1748. <https://doi.org/10.1007/s00213-018-5156-5>, PubMed: 30604184
- van Wouwe, N. C., Kanoff, K. E., Classens, D. O., Spears, C. A., Neimat, J., van den Wildenberg, W. P., et al. (2016). Dissociable effects of dopamine on the initial capture and the reactive inhibition of impulsive actions in Parkinson's disease. *Journal of Cognitive Neuroscience*, *28*, 710–723. https://doi.org/10.1162/jocn_a_00930, PubMed: 26836515
- Vo, A., Schindlbeck, K. A., Nguyen, N., Rommal, A., Spetsieris, P. G., Tang, C. C., et al. (2023). Adaptive and pathological connectivity responses in Parkinson's disease brain networks. *Cerebral Cortex*, *33*, 917–932. <https://doi.org/10.1093/cercor/bhac110>, PubMed: 35325051

- Volkow, N. D., Wang, G. J., & Baler, R. D. (2011). Reward, dopamine and the control of food intake: Implications for obesity. *Trends in Cognitive Sciences*, *15*, 37–46. <https://doi.org/10.1016/j.tics.2010.11.001>, PubMed: 21109477
- Volkow, N. D., Wang, G. J., Fowler, J. S., Logan, J., Schlyer, D., Hitzemann, R., et al. (1994). Imaging endogenous dopamine competition with [¹¹C]raclopride in the human brain. *Synapse*, *16*, 255–262. <https://doi.org/10.1002/syn.890160402>, PubMed: 8059335
- Volkow, N. D., Wang, G. J., Telang, F., Fowler, J. S., Thanos, P. K., Logan, J., et al. (2008). Low dopamine striatal D2 receptors are associated with prefrontal metabolism in obese subjects: possible contributing factors. *Neuroimage*, *42*, 1537–1543. <https://doi.org/10.1016/j.neuroimage.2008.06.002>, PubMed: 18598772
- Voon, V., Brezing, C., Gallea, C., Ameli, R., Roelofs, K., LaFrance, W. C., Jr., et al. (2010). Emotional stimuli and motor conversion disorder. *Brain*, *133*, 1526–1536. <https://doi.org/10.1093/brain/awq054>, PubMed: 20371508
- Voon, V., Hassan, K., Zurowski, M., de Souza, M., Thomsen, T., Fox, S., et al. (2006). Prevalence of repetitive and reward-seeking behaviors in Parkinson disease. *Neurology*, *67*, 1254–1257. <https://doi.org/10.1212/01.wnl.0000238503.20816.13>, PubMed: 16957130
- Voon, V., Sohr, M., Lang, A. E., Potenza, M. N., Siderowf, A. D., Whetteckey, J., et al. (2011). Impulse control disorders in Parkinson disease: A multicenter case—control study. *Annals of Neurology*, *69*, 986–996. <https://doi.org/10.1002/ana.22356>, PubMed: 21416496
- Weintraub, D., Koester, J., Potenza, M. N., Siderowf, A. D., Stacy, M., Voon, V., et al. (2010). Impulse control disorders in Parkinson disease: A cross-sectional study of 3090 patients. *Archives of Neurology*, *67*, 589–595. <https://doi.org/10.1001/archneurol.2010.65>, PubMed: 20457959
- Weintraub, D., Mamikonyan, E., Papay, K., Shea, J. A., Xie, S. X., & Siderowf, A. (2012). Questionnaire for impulsive-compulsive disorders in Parkinson's disease-rating scale. *Movement Disorders*, *27*, 242–247. <https://doi.org/10.1002/mds.24023>, PubMed: 22134954
- White, C. N., Ratcliff, R., Vasey, M. W., & McKoon, G. (2010). Using diffusion models to understand clinical disorders. *Journal of Mathematical Psychology*, *54*, 39–52. <https://doi.org/10.1016/j.jmp.2010.01.004>, PubMed: 20431690
- Wylie, S. A., Claassen, D. O., Huizenga, H. M., Schewel, K. D., Ridderinkhof, K. R., Bashore, T. R., et al. (2012). Dopamine agonists and the suppression of impulsive motor actions in Parkinson disease. *Journal of Cognitive Neuroscience*, *24*, 1709–1724. https://doi.org/10.1162/jocn_a_00241, PubMed: 22571461